ULTRASONIC CAVITATION-ASSISTED MOLTEN METAL PROCESSING OF CAST A356-NANOCOMPOSITES

Xiaoda Liu, Shian Jia, Laurentiu Nastac
Department of Metallurgical and Materials Engineering, The University of Alabama, Tuscaloosa, AL, USA

Abstract

There is strong evidence that the mechanical properties of a cast component can be considerably improved if nanoparticles are used as a reinforcement to form a metal-matrix-nano-composite (MMNC).

In this paper, Al_2O_3 and SiC nanoparticles reinforced A356 matrix composite castings were fabricated by using ultrasonic technology (UST). The A356 alloy and Al_2O_3/SiC nanoparticles were used as the matrix alloy and the reinforcement, respectively. Nanoparticles were inserted into the molten metal and dispersed by ultrasonic cavitation and acoustic streaming to avoid agglomeration. The microstructures and mechanical properties of the cast nano-composites were investigated in detail. The results showed that microstructures were greatly refined and with the addition of nanoparticles, tensile strength, yield strength and elongation increased significantly. Since the ultrasonic energy was concentrated in a small region under the ultrasonic probe, it is difficult to ensure proper cavitation and acoustic streaming for efficient dispersion of the nanoparticles without determining the suitable ultrasonic parameters via modeling and simulation. Accordingly, another objective of this paper was to develop well-controlled UST experiments that will be used in the development and validation of an UST dispersion modeling and simulation tool.

Keywords: *ultrasonic cavitation, A356-based nano-composites, ceramic nanoparticles, mechanical properties microstructure*

Introduction

Aluminum matrix composites have the potential to offer desirable properties, including low density, high specific strength, high specific stiffness, excellent wear resistance and a controllable expansion coefficient, which make them attractive for numerous applications in aerospace, automobile industry, and the military.[1–4]

During fabrication of the cast composites, it has been found that larger dendritic structures which are present during solidification may lead to particle clustering, whereas fine dendrite or regular globular structures may produce a more uniform distribution of the particles.[5-6] Hence, any processing step that can make the grain size smaller can reduce the heterogeneity of the reinforcement distribution in the solidified region, which in turn will improve the mechanical properties of the aluminum matrix composites components. Also, according to the Hall-Petch strengthening theory, the smaller the grain sizes the harder the material.

Generally, micro-ceramic particles are used to improve the yield and ultimate strength of the metal. It is of interest to use nano-sized ceramic particles to strengthen metal matrix nano-composite (MMNC), while maintaining good ductility.[7-8] Currently, there are several fabrication methods for MMNCs, including mechanical alloying with high energy milling,[9] ball milling,[10] nano-sintering,[11] vortex process,[7] spray deposition, electrical plating, sol–gel synthesis, laser deposition, etc. The mixing of nano-sized ceramic particles is lengthy, expensive, and energy consuming. The solid-state technologies discussed above that are used for manufacturing Al metal matrix composites (MMCs) suffer from size and complexity limitations of the components. The liquid-state technologies including stir-casting and compo-casting are attractive due to their low cost, high yield, and near net shaping capability. However, the stir casting process cannot disperse the nanoparticles uniformly into the melt due to their large surface-to-volume ratio and poor wettability.

Several recent studies revealed that ultrasonic vibration is highly efficient in dispersing nanoparticles into the melt.[12, 15] Ultrasonic vibration has been extensively used in: 1) purifying, degassing, and refinement of metallic melts[13–15] and 2) for introducing the ultrasonic energy into a liquid that will induce nonlinear effects such as cavitation and acoustic streaming. Ultrasonic cavitation can create small-size transient domains that could reach very high temperatures and pressures as well as extremely high heating and cooling rates. The shock force occurring during ultrasonic cavitation coupled with local high temperatures could break nanoparticle clusters and clean the surface of the particles.[16–18] Fur-

thermore, ultrasonic vibration can improve the wettability between the reinforced nanoparticles and the metal matrix, and distribute particles uniformly into the metal matrix.

Among various types of ceramic particles such as oxides, nitrides, or carbides, Al_2O_3 and SiC are widely used as reinforcement particles[19-20] due to their relatively good thermal and chemical stability as compared to other types of reinforcements.[21-22] In this article, the effects of the ultrasonically dispersed Al_2O_3 and SiC nanoparticles on the as-cast microstructure are studied.

Experimental Setup and Procedure

Materials Used in Experiments

Aluminum alloy A356 (Table 1) was selected as the metallic matrix because it is readily castable and widely used. The ceramic nanoparticles used in this study were β-SiC (spherical shape, average diameter of about 50 nm) and Al_2O_3 (spherical shape, average diameter of about 20 nm).

Experimental Setup

Figure 1 shows the ultrasonic processing system at the Solidification Laboratory, at the University of Alabama at Tuscaloosa. The main parameters of the ultrasonic equipment are: maximum power, P=2.4 kW and frequency, f =18 kHz. An induction furnace with a capacity of 6 lb (2.7 kg) was used to melt the A356 alloy. A quartz tube with an adjustable switch was used to inject the ceramic nanoparticles, and the nanoparticles were blown into the melt by Ar gas. The nanoparticles can be injected into the melt slowly under control and no air contamination was guaranteed. The A356 molten pool was protected by Argon gas atmosphere at the same time. A temperature probe was used to monitor the melt temperature to control the superheat. The permanent metal mold (as shown in Figure 1b) can be preset to a well-controlled temperature in order to study the effects of different mold temperature and cooling rates. The specimen extracted from the metal mold (as shown in Figure 1b) was tested on the tensile test machine. The dimensions of the specimen are 2 inches (5.08 cm) length and 0.5 inch (1.27 cm) diameter. The parameters of the ultrasonic stirring technology were determined using an ultrasonic technology (UST) software tool previously developed and validated.[23] The UST analysis tool is capable to model acoustic streaming and cavitation.

Experimental Procedure

A brief description on the experimental procedure is as follows:

1. Preheat the permanent metal mold to the desired temperature.
2. Weigh and preheat the A356 ingots (5 lb [2.3 kg]) to eliminate any moisture and other contaminants, and then add them to the furnace for melting.
3. After the alloy is melted, insert the Nb (Niobium) ultrasonic probe about 2 inches (5.08 cm) beneath the melt surface, perform ultrasonic stirring at 1.75 kW (about 70% of the maximum power-2.4kW) and 18 kHz frequency (determined by the current UST

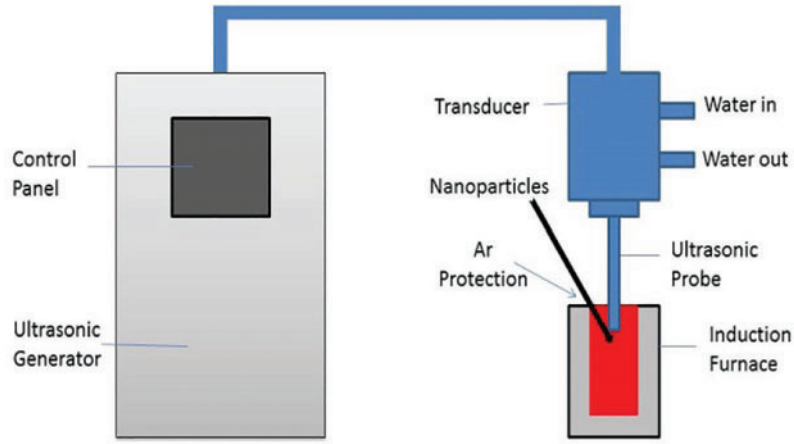

(a) Ultrasonic Processing System

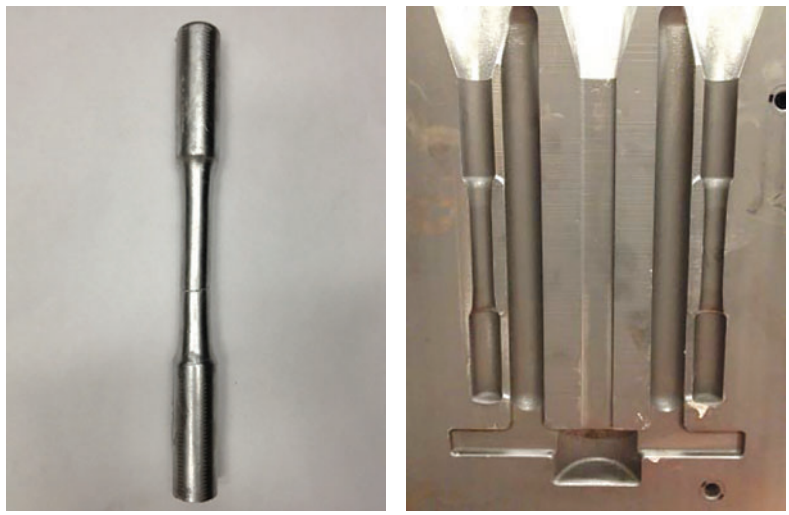

(b) Metal Mold and Test Specimen

Figure 1. UST-induction furnace equipment (a) and metal mold and test specimen (b), which were used at the Solidification Laboratory, University of Alabama, Tuscaloosa.

Table 1. Nominal Chemical Composition of Matrix Alloy A356

Element	Si	Fe	Cu	Mn	Mg	Zn	Ti	Al
wt. %	6.5-7.5	0.20	0.20	0.10	0.25-0.45	0.10	0.20	balance

equipment), as shown in Figure 1. The utilized power is sufficient to create cavitation into the melt.

4. A quartz tube was inserted into the melt, in the cavitation area; Ar was applied to insert Al_2O_3/SiC nanoparticles into the melt. 0.7 wt.% and 1 wt.% SiC and 1 wt.% Al_2O_3 nanoparticles were added during a 5 minute time-frame. Note that the UST processing time was 15 min.
5. A higher pouring temperature of 1382°F (750°C) was used to minimize the formation of metal-mold filling defects including cold-shuts. The metal mold was preheated to about 752°F (400°C).
6. The casting was extracted from the metal-mold after cooling in the mold for at least 30 min.
7. A small sample was extracted for microstructure analysis.

Results and Discussion

Optical Microstructure Analysis

Figures 2-4 show the microstructures of the A356 alloy cast in the metal molds at magnifications of 50x, 200x and 1000x, respectively. From these pictures, it is clear that the grains were refined after the ultrasonic treatment when compared to the sample without any treatment. Also, the grain size of the samples with nanoparticles are smaller than the samples without them. In addtion, a comparision between Figure 2(c) and 2(d) showed that with the increase in the weight percent of the SiC nanoparticles, the grain sizes become even smaller. The reason for this decrease might be because the dispersed nanoparticles block the grains from growing larger (e.g., impingement effect of nanoparticles on grain growth). In addition, the more nanoparticles in the melt, the less space for the grains to grow, so the grains should become finer. According to Table 2, the secondary dendrite arm spacing (SDAS) decreased by 11.3% after ultrasonic treatment, and with the addition of nanoparticles, SDAS even decreased by more than 36.2% than in the standard A356 alloy. Also, the eutectic structures are more refined after UST processing (see Figure 4). In addition, the amount of porosities after ultrasonic treatment has been reduced significantly. The degassing effect of the ultrasonic treatment is clearly shown in Figures 2-4.

According to Hall-Petch strengthening theory:

$$\sigma_y = \sigma_0 + \frac{k_y}{\sqrt{d}} \qquad \text{Eqn. 1}$$

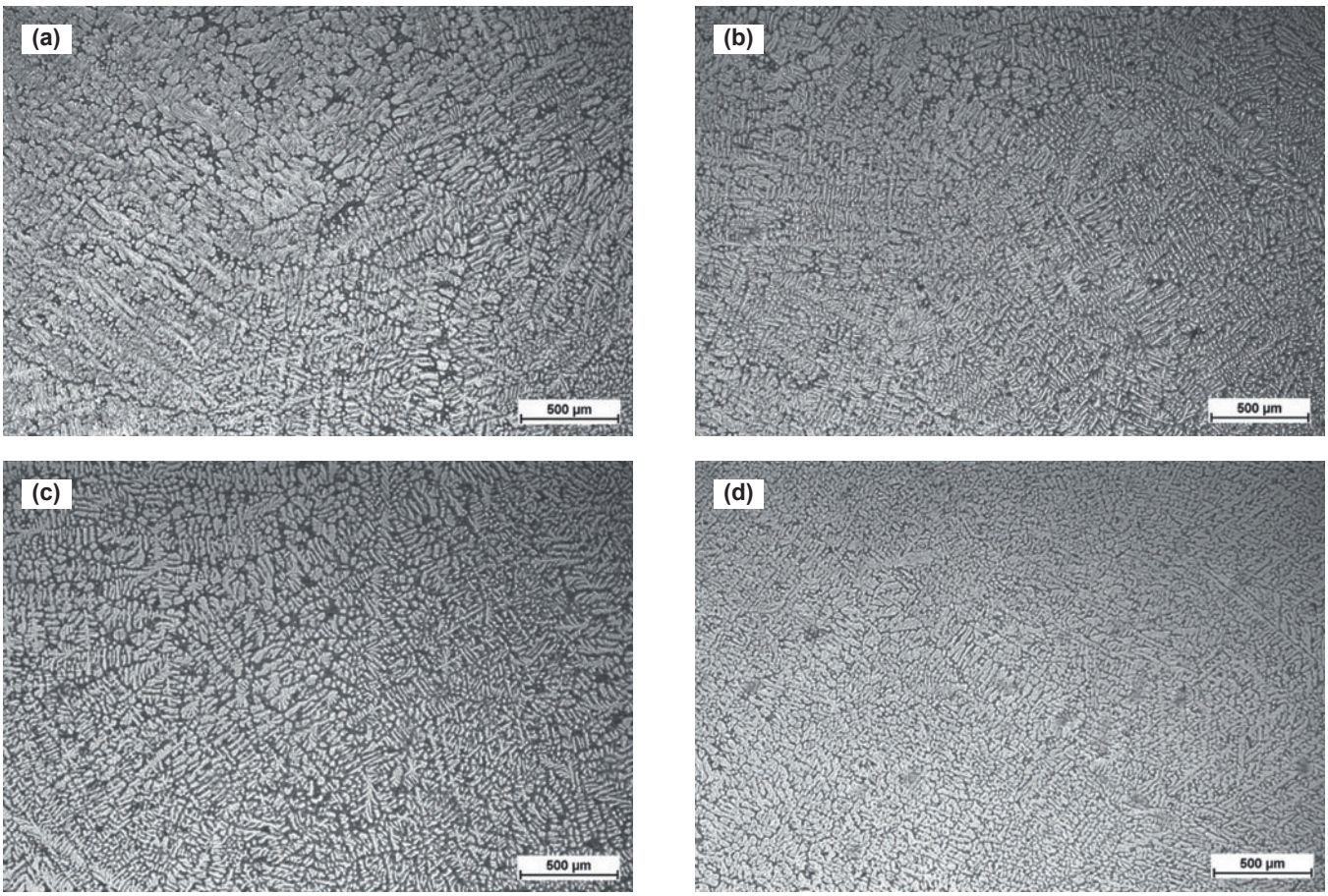

Figure 2. Microstructures of A356 alloy under magnification of 50X (metal-mold samples): (a) Standard (without UST) (b) UST+Al_2O_3 (c) UST+0.7%SiC (d) UST+1%SiC.

Where σ_y is the yield stress, σ_o is a materials constant for the starting stress for dislocation movement (or the resistance of the lattice to dislocation motion), k_y is the strengthening coefficient (a constant unique to each material), and d is the average grain diameter or average arm spacing of the microstructure under consideration.

A more detailed equation with the addition of eutectic phase fraction, f_E, can be written as follows:

$$\sigma = f_p \cdot \sigma_p + f_E \cdot \sigma_E \qquad \text{Eqn. 2}$$

where σ is the overall mechanical yield strength, f_p is the fraction of primary dendritic phase, f_E is the fraction of eutectic phase , σ_p is the yield stress of primary dendritic phase, σ_E is the yield stress of eutectic phase. Both σ_p and σ_E are inversely proportional to the size of microstructure as shown by Eqn. 1.

As shown by Eqns. 1 and 2, the strength will increase when the dimensions of the primary and euctectic phases decrease. This is also verified by the current experimental measurements (see Table 2).

SEM Analysis of A356/1wt% SiC Sample

Figure 5 shows the distribution of SiC nanoparticles in the A356/1wt% SiC MMNC sample. It can be seen that SiC nanoparticles were well dispersed into the A356 matrix. It also showed that some agglomeration had occurred during the MMNC processing. Further analysis is required to determine the cause of this agglomeration and how to prevent it.

To double check the SiC distribution in the nanocomposite, energy dispersive X-ray spectroscopy (EDS) analysis was also performed. Figure 6 shows the EDS spectrum of the

Table 2. Comparison of SDAS Measured in the Processed Samples

SDAS (μm)	1	2	3	Average
Standard A356	23.2	28.0	32.1	**27.8**
UST+Al_2O_3	20.6	19.1	11.7	**17.1**
UST+0.7%SiC	16.7	24.0	12.8	**17.8**
UST+1%SiC	15.7	15.0	15.1	**15.3**

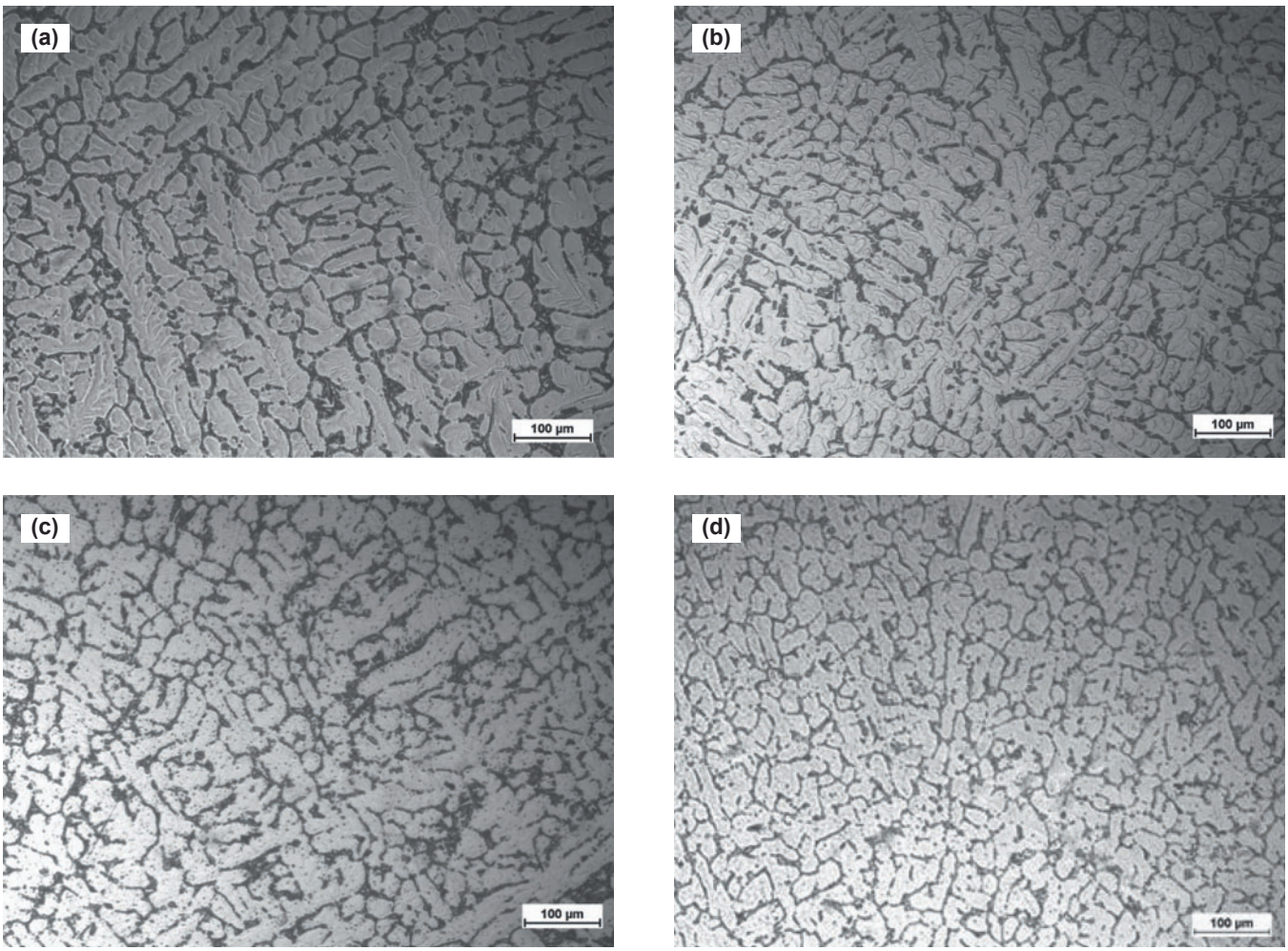

Figure 3. Microstructures of A356 alloy under magnification of 200X (metal-mold samples): (a) Standard (without UST) (b) UST+Al_2O_3 (c) UST+0.7%SiC (d) UST+1%SiC.

carbon distribution in the A356 nanocomposites. From the carbon distribution shown in Figure 6, a uniform dispersion of SiC nanoparticles can be assumed. Further scanning electron microscopy (SEM) and transmission electron microscopy (TEM) analyses will be carried out to better understand the SiC dispersion into the A356 matrix.

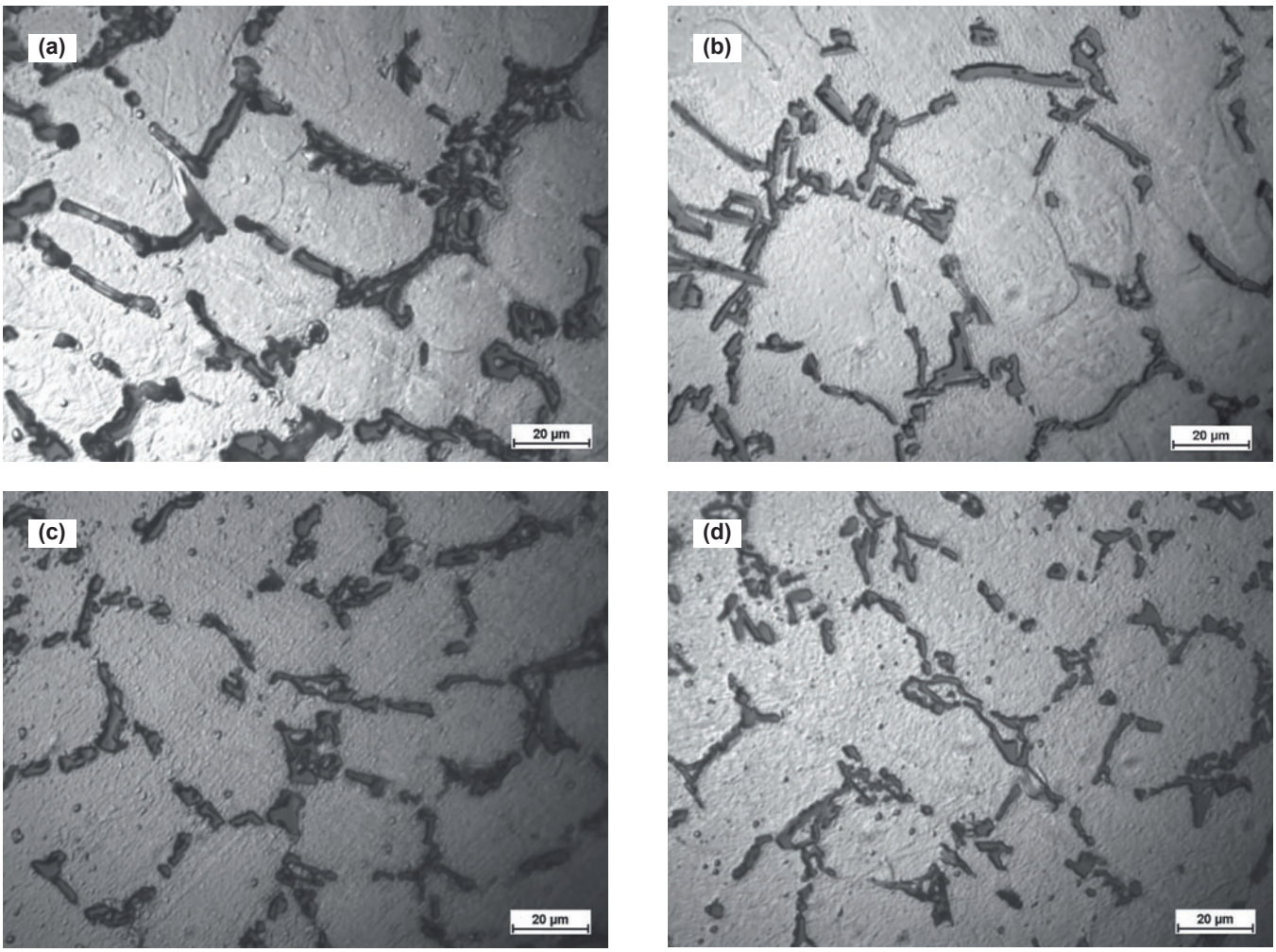

Figure 4. Eutectic microstructures of A356 alloy under magnification of 1000X (metal-mold samples): (a) Standard (without UST) (b) UST+Al_2O_3 (c) UST+0.7%SiC (d) UST+1%SiC.

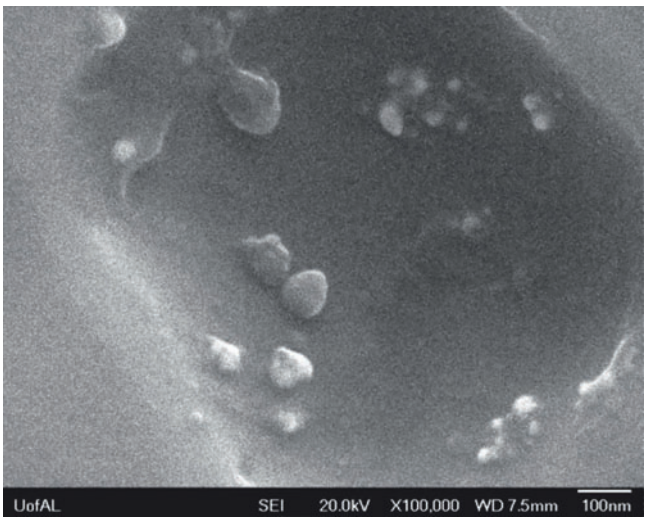

Figure 5. The distribution of SiC nanoparticles in the MMNC sample.

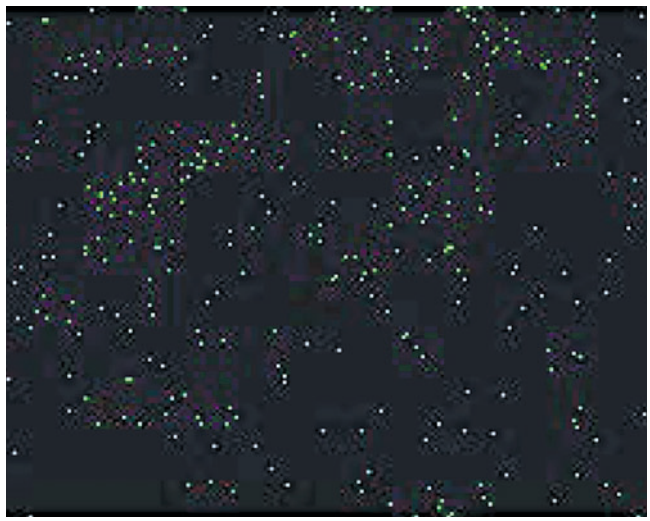

Figure 6. EDS mapping showing carbon distribution in the nanocomposite material.

Table 3. Comparison of Tensile Properties Measured in the Processed Samples

Samples	Tensile Strength(MPa)	Yield Strength(MPa)	Elongation (%)
Standard A356(without UST, Ar degassing for 3 min.)	228 ± 4	180 ± 3	4.0 ± 0.3
UST 5min +1% Al_2O_3	263 ± 8	196 ± 5	6.3 ± 0.5
UST+1% SiC	283 ± 4	196 ± 2	11.2 ± 0.9
Remelt UST+1% SiC	275 ± 7	190 ± 6	6.3 ± 0.3

Analysis of Mechanical Properties

After the T6 heat treatment, solution heat treatment for 4h at 932°F (500°C) and aging heat treatment for 4h at 311°F (155°C), mechanical testing was done to evaluate tensile strength, yield strength and elongation, see Table 3. The addition of the nanoparticles increased the tensile strength by 15.3%, 24.1%, 20.7%, respectively. For the tensile tests shown in Table 3, three samples were tested and the average value was considered.

At the same time, improvement in elongation can be seen as well in all UST+nanoparticles samples. Furthermore, the A356+SiC nanocomposites performed slightly better than the A356+Al_2O_3, perhaps due to the fact that the samples with Al_2O_3 nanoparticles have more gas pores than the ones with SiC nanoparticles (Figure 3). These phenomena can be explained by the fact that aluminum is easy to oxidize and after oxidation, the wettability between aluminum and Al_2O_3 nanoparticles became worse. Note also that the tensile properties of the remelt samples (UST+1%SiC) were higher than those of the standard A356 alloy, which were obtained using prime A356 material (without UST, Ar degassing for 3 min.). This suggests that the SiC nanoparticles remained well-dispersed during the remelt process.

Conclusions and Future Work

Two main effects of ultrasonic treatment can be seen from the experiments:

1. Due to ultrasonic treatment, microstructures were refined by ultrasonic stirring and cavitation; grain size and SDAS decreased, columnar-to-equiaxed-transition (CET) was completely eliminated;
2. Ultrasonic degassing of the molten alloy was quite qood; this is demonstrated by the observed reduced gas porosity in all samples in Figures 2-4.

By using SEM and EDS analyses, it was shown the nanoparticles were well dispersed in the nanocomposites; but some agglomeration still exists.

Significant improvement in the mechanical properties including tensile strength and yield strength as well as ductility were achieved after adding the ceramic nanoparticles by ultrasonic processing.

Future work will include scanning transmission electron microscopy (STEM) analysis of cast A356 nano-composites to clearly understand the effects of ultrasonic cavitation process on dispersion of nanoparticles and whether the dispersion of nanoparticles is uniform or not after the ultrasonic cavitation and acoustic streaming processing.

In addition, a computational fluid dynamics model that can simulate the ultrasonic processing of nano-composites, which was recently developed[23,24] will be soon validated using the UST-experimental results at the University of Alabama, Solidification Laboratory.

REFERENCES

1. Su, B., Yan, H.G., Chen, G., Shi, J.L., Chen, J.H., Zeng, P.L., "Study on the Preparation of the SiCp/Al-20Si-3Cu Functionally Graded Material Using Spray Deposition," Mater. Sci. Eng. A, vol. 527, issues 24-25, pp.6660-6665 (2010).
2. Seyed Reihani, S.M., "Processing of Squeeze Cast Al6061-30vol% SiC Composites and Their Characterization," Mater. Des., vol. 27, issue 3, pp. 216–222 (2006).
3. Bozic, D., Dimcic, B., Dimcic, O., Stasic, J., Rajkovic, V., "Influence of SiC particles Distribution on Mechanical Properties and Fracture of DRA Alloys," Mater. Des., vol. 31, issue 1, pp. 134-141 (2010).
4. De Cicco, M.P., Li, X., Turng, L-S., "Semi-Solid Casting (SSC) of Zinc Alloy Nanocomposites," J. Mater. Process. Technol., vol. 209, issues 18-19, pp. 5881–5885 (2009).
5. Eskin, G.I., "Principles of Ultrasonic Treatment: Application of Light Alloy Melts,"Adv. Perform. Mater., vol. 4, issue 2, pp. 223–232 (1997).

6. Jian, X., Xu, H., Meek, T.T., Han, Q., "Effect of Power Ultrasound on Solidification of Aluminum A356 Alloy," Mater. Lett., vol. 59, pp. 190–193 (2005).
7. Akio, K., Atsushi, O., Toshiro, K., Hiroyuki, T., "Fabrication Process of Metal Matrix Composite with Nano-Size SiC Particle Produced by Vortex Method," J. Jpn. Inst. Light Met., vol. 49, pp. 149–154 (1999).
8. Mussert, K.M., Vellinga, W.P., Bakker, A., Van Der Zwaag, S., "A Nano-Indentation Study on the Mechanical Behaviour of the Matrix Material in an AA6061 - Al_2O_3 MMC," J. Mater. Sci., vol. 37, issue 4, pp. 789–794 (2002).
9. Chen, X., Baburaj, E.G., Froes, F.H., Vassel, A., "Ti-6Al-4V/SiC Composites by Mechanical Alloying and Hot Isostatic Pressing," Proceed. Adv. Particulate Materials and Processes – Int'l Conference, Publisher: Metal Powder Industries Federation, Princeton, NJ, pp. 185–192 (1997).
10. Urtiga Filho, S.L., Rodriguez, R., Earthman, J.C., Lavernia, E.J., "Synthesis of Diamond Reinforced Al-Mg Nanocrystalline Composite Power Using Ball Milling," Mater. Sci. Forum, vols. 416–418, pp. 213–218 (2003).
11. Groza, J.R. "Sintering of Nanocrystalline Powders," Int. J. Powder Metall., vol. 35, pp. 59–66 (1999).
12. Habibnejad-Korayem, M., Mahmudi, R., Ghasemi, H.M., Poole, W.J., "Tribological Behavior of Pure Mg and AZ31 Magnesium Alloy Strengthened by Al_2O_3 Nano-particles," Wear, vol. 268, pp. 405-412 (2010).
13. Mula, S., Padhi, P., Panigrahi, S.C., Pabi, S.K., Ghosh, S., "On Structure and Mechanical Properties of Ultrasonically Cast Al-2% Al_2O_3 Nanocomposite," Mater. Res. Bull., vol. 44, pp. 1154–60 (2009).
14. Wielage, B., Hoyer, I., Weis, S., "Soldering Aluminum Matrix Composites," Weld. J., vol. 86, pp. 67-70 (Mar. 2007).
15. Xu, Z.W., Yan, J.C., Wu, G.H., Kong, X.L., Yang, S.Q., "Interface Structure and Strength of Ultrasonic Vibration Liquid Phase Bonded Joints of Al_2O_{3p}/6061Al Composites," Scripta Mater., vol. 53, issue 7, pp. 835–839 (2005).
16. Lan, J., Yang, Y., Li, X.C., "Microstructures and Microhardness of SiC Nanoparticles Reinforced Magnesium Composites Fabricated by Ultrasonic Method," Mater. Sci. Eng. A, vol. 386, pp. 284–290 (2004).
17. Cao, G., Choi, H., Konishi, H., Kou, S., Lakes, R., Li, X., "Mg-6Zn/1.5% SiC Nanocomposites Fabricated by Ultrasonic Cavitation-based Solidification Processing," J. Mater. Sci., vol. 43, issue 16, pp. 5521–5526 (2008).
18. Yan, J.C., Xu, Z.W., Shi, L., Ma, X., Yang, S.Q., "Ultrasonic Assisted Fabrication of Particle Reinforced Bonds Joining Aluminum Metal Matrix Composites," Mater. Des., vol. 21, issue 1, pp., 343–347 (2011).
19. Yang, Y., Lan, J., Li, X., "Study on Bulk Aluminum Matrix Nano-Composite Fabricated by Ultrasonic Dispersion of Nano-Sized SiC Particles in Molten Aluminum Alloy," Mater. Sci. Eng. A, vol. 380, issues 1-2, pp. 378-383 (2004).
20. Li, X., Yang, Y., Weiss, D., "Theoretical and Experimental Study on Ultrasonic Dispersion of Nanoparticles for Strengthening Cast Aluminum Alloy A356," Metall. Science and Tech., vol. 26, no.2 (2008).
21. Ying, D.Y., Zhang, D.L., "Processing of Cu-Al_2O_3 Metal Matrix Nanocomposite Materials by Using High Energy Ball Milling," Mater. Sci. Eng. A, vol. 286, issue 1, pp. 152–156 (2000).
22. Kok, M., "Production and Mechanical Properties of Al_2O_3 Particle-Reinforced 2024 Aluminium Alloy Composites," J. Mater. Process. Technol., vol. 161, pp. 381–387 (2005).
23. Nastac, L., "Mathematical Modeling of the Solidification Microstructure Evolution in the Presence of Ultrasonic Stirring," Metall. Mater. Trans. B, vol. 24, pp. 1297-1305 (2011).
24. Nastac, L., "Multiscale Modeling of the Solidification Microstructure Evolution in the Presence of Ultrasonic Stirring," IOP Conf. Ser.: Mater. Sci. Eng. vol. 33 012079 (June 2012).

Technical Review and Discussion on next page.

Ultrasonic Cavitation-Assisted Molten Metal Processing of Cast A356-Nanocomposites

Xiaoda Liu, Shian Jia, Laurentiu Nastac;
The University of Alabama, Tuscaloosa, AL, USA

Reviewer: Previous review have questioned this statement on aspect that Hall-Petch strengthening, that smaller grains would result in harder material. Is that the resulting change in material properties or is it strengthening?

Authors: *We do not know exactly how the mechanical properties are improved. Both change in material properties and strengthening may contribute to the increase in mechanical properties. Further research is needed in this area.*

Reviewer: Previous papers [1-7] have unanimously used 20 kHz for the resonant frequency of ultrasonic processing. Recent studies by Borgonovo and Makhlouf [1] during tuning of ultrasonic probes for metal degassing have shown the importance of the resonant frequency. The optimum value has been found to lie between 20 and 20.56 kHz for a 1.75 kW power usage. This has not been addressed in this paper.

Authors: *Indeed, the reviewer is right in stating that a frequency of 20 KHz is optimum. The ultrasonic equipment used in this study was tuned for 18 KHz and the frequency could not be changed. The alloy type should change this resonant frequency. Also, based on equation 1 below, ultrasonic intensity further from the probe is acceptable. The author also performed ultrasonic cavitation modeling for the ultrasonic system at UA and found that cavitation still takes place at 18Khz. The ultrasonic intensity, I_{us}* (in W/m^2) *can be calculated as below. (L. Nastac, "Modeling and Simulation of Microstructure Evolution in Solidifying Alloys"; published by Springer, 2004).*

$$I_{us} = 0.5\, a^2\, \omega^2\, \rho\, v\, \exp(-\alpha x) = I_{us}^{o}\, \exp(-\alpha x)$$
$$\text{with} \quad \alpha = C\,\frac{f^2}{v^3\,\rho}\,\eta \qquad [1]$$

In Equation (1) ρ *is the material density,* ω *is the angular frequency,* η *is the material viscosity, I_{us}^{o} is the reference ultrasonic intensity at x = 0, f is the sound frequency, v is the velocity,* a *is the amplitude of the oscillations,* α *is the absorption coefficient, C is a material constant, and x is the distance. For metals, for example for f* = 20 kHz, α *is of the order of* 10^{-6} [m^{-1}].

In the paper we mentioned the following: "…18 kHz frequency (determined by the current UST equipment."

Reviewer: Can you comment about the use of induction field vs. use of resistance melting?

Authors: *We believe that the use of induction melting in the presence of ultrasonic stirring provides better results, that is, the dispersed nano-particles from the cavitation area will be mixed quicker with the bulk liquid that in the case when resistance melting is used. The UST processing time is about 15 min with induction melting. We expect much longer UST processing time when using the resistance melting.*

Reviewer: What was the gas flow rate/velocity used?

Authors: *A special equipment/process was used to add the nanoparticles into the melt. The equipment/process information is proprietary (and patentable) and unfortunately, cannot be disclosed in this paper.*

Reviewer: Can you explain why the use of C Ka1_2 line is appropriate for mapping nano-composite distribution

Author: *Since C is not a matrix element in A356 alloy, the common sense is to use its distribution for mapping SiC distribution.*

Reviewer: Why was such a low solution temperature selected? This not a normal temperature, which is 540C. What was the quenchant used– cold water, hot water?

Authors: *This Heat treatment is not really optimized; further work is required. The quenchant was warm water.*

Reviewer: There is no tensile property data listed for the 0.7% samples.

Authors: *The tensile testing was done only on the A356-1%SiC (better microstructure than the A356-1%SiC). Further work will be done soon to study the effect of the amount of SiC nanoparticles on mechanical properties. Note also that the tensile properties of the remelt samples (UST+1%SiC) were higher than those of the standard A356 alloy, which were obtained using prime A356 material (without UST, Ar degassing for 3 min). This suggests that the SiC nanoparticles remained well-dispersed during the remelt process.*